NUMERICAL SIMULATION OF THE EFFECT OF DIAPHRAGM ORIFICE DIAMETER IN A FLAMEPROOF ENCLOSURE WITH AN INTERCONNECTED STRUCTURE DURING PRESSURE PILING

by

Dong LI[a,b*] and Shijie DAI[a]

[a] School of Mechanical Engineering, Hebei University of Technology, Tianjin, China
[b] CNOOC Tianjin Chemical Research and Design Institute Ltd, Tianjin, China

Original scientific paper
https://doi.org/10.2298/TSCI220613137L

Combustible gas explosions are typically triggered at high temperatures by the generation of electric sparks on starting, stopping, or short circuiting of electrical equipment. Flameproof enclosures are widely installed in the petrochemical industry as safety equipment for eliminating ignition sources. Such enclosures are designed with a double-cavity structure, and a hole plate is used to connect the two cavities. However, pressure piling occurs in such double-cavity-connected structures, resulting in flameproof enclosures requiring to bear higher pressure than designed, which is a safety hazard. However, few studies have focused on the effect of the diaphragm orifice diameter of flameproof enclosures. Because the explosion of combustible gas in a flameproof enclosure is a complex process, numerical simulation was performed to study the process. Fluent was used for numerically simulating the ethylene/air premixed gas explosion characteristics of double-cavity-connected structure flameproof enclosures. The effects of an orifice hole diameter from 10 mm to 45 mm on flameproof characteristics, including the maximum explosion pressure, maximum explosion pressure rise rate, and maximum explosion index, were examined. The results are critical for the effective design of a double-cavity flameproof shell and provide theoretical support for fire suppression in a flameproof enclosure.

Key words*: pressure piling, orifice, numerical simulation, FLUENT*

Introduction

Explosive mixtures entering the interior of enclosures through any joint or structural gap of the enclosure can cause explosions. However, flameproof structures avoid internal damage and ignition of an explosive gas environment formed by one or more gases or vapors [1]. The explosion-proof performance, which is the ability of the enclosure to withstand an internal explosion and exhibit limited damage and deformation, is a critical parameter of a flameproof enclosure. [2]. Flameproof enclosures are widely installed in the petrochemical industry with explosive hazards to achieve electrical functions and satisfy process requirements. When switches and high temperature devices are installed inside flameproof enclosures, a double-cavity structure connected by an orifice with a small hole is used for safety and ease of installation. However, this design structure is prone to pressure piling, and in case of an explosion, the pressure becomes considerably higher than thermodynamic calculation considered for the structure during design [3-6]. A flameproof enclosure designed for normal pressure can be eas-

* Corresponding author, e-mail: lidong@pcec.com.cn

ily destroyed. This explosion mechanism is a major risk in industry because of the presence of flammable gases [7]. Therefore, the design of a flameproof enclosure for studying the influence of orifice holes on the pressure piling of the flameproof enclosures with the double-cavity-connected structure is critical.

Pressure piling is defined as ignition in one cavity or compartment of a shell, which triggers an explosion of a pre-compressed gas mixture in the other cavity or compartment [2]. Numerous experimental and numerical studies on pressure piling have focused on a connected device and considered the initial pressure, container-length-to-diameter ratio, and pipe diameter as boundary conditions. Razus *et al.* [8] studied connected devices consisting of cylindrical vessels of volumes 1180 cm^3 and 170 cm^3 and pipes of lengths 4.35 cm (inner diameter: 3.0-8.3 cm) and revealed that the pipe diameter was the primary factor affecting the explosion of the connected device, and the explosion pressure increased with the decrease in the pipe diameter. Zhen *et al.* [9] investigated the influence of the initial pressure on the explosion pressure of the connected pipes using a connected device composed of spherical vessels with volumes of 0.113 m^3 and 0.022 m^3 and two pipes of lengths 2 m and inner diameter 0.06 m. The experimental results revealed that the explosion pressure increased linearly with the increase in the initial pressure. Ogungbemide *et al.* [10] used connected devices composed of cylindrical containers with volumes of 0.025 m^3 and 0.006 m^3 and pipes of length 1.0 m (inner diameter: 0.04 m) to simulate a coal dust explosion. They investigated the influence of the change of the aspect ratio (L/D) of the main container on pressure piling. Numerical simulation was performed to reproduce the four stages of a dust explosion in a closed connection system and the process of pressure piling. In a subsequent experiment, Ogungbemide *et al.* [11] conducted numerical simulation investigate the influence of the pipe bending angle on the pressure piling in the dust explosions of fully enclosed interconnected vessels and revealed that pressure piling was most obvious when the bending angle was 0 °C. With the increase in the bending angle, the maximum pressure value and pressure rise rate decreased.

The pressure piling of flameproof enclosures is typically studied using experimental methods. Kumar *et al.* [12] studied two identical shells connected with a pipe diameter of 1.2 or 0.3 cm and revealed that the explosion of the second shell when the pipe diameter was 1.2 cm was larger than that when the pipe diameter was 0.3 cm. However, the maximum explosion pressure rise time of the second shell exhibited the opposite trend. Krause *et al.* [13] studied a flameproof enclosure under static and dynamic pressure conditions and revealed that when pressure piling occurs, pressure and strain are not proportional. Under insufficient damping of the mechanical load or if the load corresponding to the natural frequency of the enclosure, dynamic stress is highly relevant. Munro *et al.* [14] studied flame propagation during pressure piling at low temperatures. Although the International Electrotechnical Commision standard states hydrogen to be used as an experimental gas, the designed sample experiment proved that using hydrogen as an experimental gas was not feasible to prove non-detonation at low temperatures. Therefore, ethylene was used as an experimental gas because of a higher probability of detonation at lower temperatures. Chen [15] investigated the wiring cavity effect on an explosion pressure motor. The state of the rotation of a flameproof motor was analyzed for enhancing turbulence. Under heavy turbulence, the flame winding deformation could increase the contact area of the reactant, speed up the flammable and non-flammable mixing, and intensify the heat transfer and transport rate of the reactants. Furthermore, the propagation velocity of the flame wave along the normal direction increased, and the explosion pressure value increased.

Numerous studies have focused on combustible material explosion during pressure piling to solve practical engineering problems. However, most studies on pressure piling of

flameproof enclosures have been conducted experimentally, few reports have focused on pressure piling using numerical simulation of flameproof enclosures. Pressure piling is a complex process, and recording the process experimentally is difficult. Numerical simulations can overcome the drawbacks of the experimental method. Studies have revealed that instead of the length of the connecting pipe, pressure piling is influenced by the volume ratio of the container and the diameter of the connecting pipe. For a flameproof enclosure, for a given volume of double cavity, the small hole of the orifice is the most critical factor for the pressure piling of flameproof enclosures. However, this factor is yet to be investigated in existing literature. The maximum explosion pressure, maximum rate of pressure rise, and the gas deflagration index are crucial safety parameters for assessing the flammable hazards of chemical processes, designing explosion-proof vessels, or designing vents [16]. In this study, numerical simulation was used to study the influence of the diaphragm orifice diameter on the maximum explosion pressure, maximum pressure boost speed, and maximum explosion index of a double-cavity-connected structure flameproof enclosure during pressure piling. The results of the study can provide considerable insight into the development of effective design paradigm flameproof enclosures.

Numerical simulation method

Physical model

Figure 1 displays the flameproof enclosure with a double-cavity-connected structure used for study the influence of the diaphragm orifice diameter on the pressure piling of a flameproof enclosure. Two flameproof enclosures and an orifice with a small hole in the middle were used for the study. Hexagonal bolts were used to connect the three parts. The volume of flameproof enclosure A, B, and C were 5.12 L and 10.23 L, respectively. The inner diameter for the two flameproof enclosures was 161.5 mm, and the length ratio was 1:2. Six working conditions with varying diameters were designed in the study. The diameter of the orifice hole in working conditions 1, 2, 3, 4, 5, and 6 were 10 mm, 15 mm, 20 mm, 25 mm, 30 mm, and 45 mm, respectively. The orifice is displayed in fig. 2. According to the experimental parameters and procedures specified in IEC 60079-1 ethylene was used as a typical explosive gas. Standard ambient conditions of 100000 pa pressure, 293.15 K ambient temperature, and 40% humidity were used. The flameproof shell was filled with 8 ± 0.5% ethylene by volume to air at a standard atmospheric pressure, and the premixed gas was ignited [1].

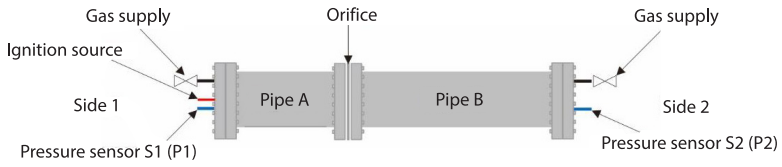

Figure 1. Flameproof housing configuration

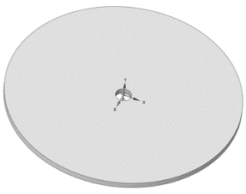

Figure 2. Orifice

Calculation domain

The parameters of the axial and radial directions of fluid changes are critical from the perspective of an axisymmetric geometry structure. Therefore, domain modelling was performed, and a 2-D axisymmetric model was used to divide the grid and perform numerical simulations. The Boolean operation was used for dividing the grid into a structured grid, and in the holes and flameproof shell near the wall boundary-layer encryption, a quadrilateral mesh was used to divide the computing domain.

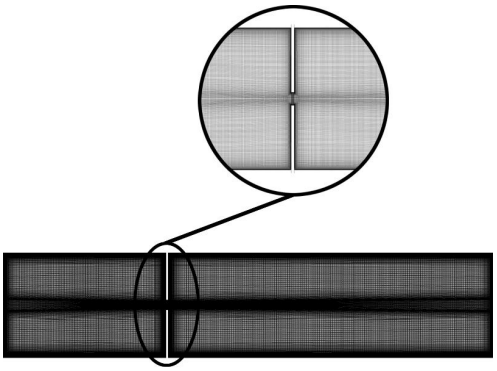

Figure 3. Grid division of computing domain

The simulation grid was encrypted several times for verifying the independence of the grid, and the results were compared with the experimental value. The grid division is displayed in fig. 3. The maximum grid size was 1 mm, and the grid size at the boundary-layer encryption was 0.15 mm. A total of 77552 structured body grids, 156029 surface grids, and 78748 nodes were presented in the 2-D axisymmetric model. The overall mass was greater than 0.2 and the aspect ratio was less than 100 (larger at the boundary-layer), which satisfied the requirements of high precision numerical simulation.

Boundary conditions

As displayed in fig. 1, flameproof enclosures *A* and *B* were filled with 8 ±0.5% ethylene by volume in relation air at the standard atmospheric pressure. The settings of the initial conditions for the combustible gas are as follows. The ambient pressure was 1 bar, the ambient humidity was 40%, and the ambient temperature was 283.15 K. For the six working conditions, the ignition position was set in the middle of the end cover of flameproof enclosure A, and the temperature was set to be 300 K. Monitoring points were set at the end cover of flameproof enclosure A, the end cover of flameproof enclosure B, and the small hole of the flameproof enclosure to monitor the pressure, temperature, and speed. The boundary conditions used in this study are presented in tab. 1.

Table 1. The boundary conditions

Parameter	Value
Fluid	Ethylene
Ambient Humidity [%]	40
Ambient Temperature [K]	293.15
Ambient pressure [bar]	1.01
Temperature (fluid) [K]	293.15
Ignition temperature [K]	300
Wall surface	Adiabatic

Model

The single-step reaction mechanism parameters of ethylene and air premixed gas combustion are presented in tab. 2. Here, A_r is the Arrhenius pre-exponential factor, n_r – the temperature coefficient, and $E_{a,r}$ [Jkg^{-1}mol^{-1}] – the activation energy.

Table 2. Single-step reaction model parameters

Reaction	A_r	n_r	$E_{a,r}$
$C_2H_4 + 3O_2 = 2CO_2 + 2H_2O$	$1.125 \cdot 10^{10}$	0	$1.256 \cdot 10^{8}$

The transient 2-D axisymmetric model was used for numerical simulation. Here, the *k-ε* turbulence equation was divided into three models, namely the standard *k-ε* (SKE) model, the RNG *k-ε* model and the reality-based realizable *k-ε* (RKE) model, depending on the method

of calculating viscosity, the Prandtl number controlling the turbulent diffusion, and the dissipation term. Among these three models, the RKE exhibited the widest adaptability and most accurate calculation.

The reality-based k-ε (RKE) turbulence control equation:

$$\frac{\partial(\rho k)}{\partial t}+\nabla(\rho k\boldsymbol{\upsilon})=\nabla\left[\left(\mu+\frac{\mu_t}{\sigma_k}\right)\nabla k\right]+G_k-\rho\varepsilon-Y_M \tag{1}$$

$$\frac{\partial(\rho\varepsilon)}{\partial t}+\nabla(\rho\varepsilon\boldsymbol{\upsilon})=\nabla\left[\left(\mu+\frac{\mu_t}{\sigma_\varepsilon}\right)\nabla\varepsilon\right]+\rho C_{1\varepsilon}-\rho C_2\frac{\varepsilon^2}{k+\sqrt{\nu\varepsilon}}+C_{1\varepsilon}\frac{\varepsilon^2}{k}C_{3\varepsilon}G_b \tag{2}$$

where ρ is the density, k – the turbulence kinetic energy, $\boldsymbol{\upsilon}$ – the speed vector, μ – the dynamic viscosity, μ_t – the turbulent viscosity, ε – the turbulence dissipation rate, G_k – the kinetic energy of turbulence caused by the mean velocity gradient, Y_M – the effect of turbulent fluctuating expansion on the total dissipation rate, μ – the dynamic viscosity, $\sigma_\varepsilon = 1.2$, $C_{1\varepsilon} = 1.44$, $C_2 = 1.9$, $C_{3\varepsilon} = 1.92$, and G_b is the kinetic energy of turbulence caused by buoyancy.

Results and discussion

Verification of numerical simulation results

Because of limited experimental data in the literature on the effect of various diaphragm orifice diameters on the explosion parameters of the double-cavity connected structure flameproof enclosure during pressure piling, the experimental data of Zhang *et al.* [5] were compared with the numerical simulation results of ignition on the right side with the diaphragm orifice diameter of 15 mm. The maximum explosion pressure reported by Zhang *et al.* [5] was compared with the numerical simulation result, tab. 3, which revealed that the numerical simulation result was slightly lower than the experimental value, which was attributed to the deviation of the ethylene gas concentration and ignition energy. To verify the reliability of numerical simulation, the numerical simulation explosion pressure curve was compared with the experimental curve reported by Zhe *et al.* [6], fig. 4. The maximum explosion pressure in numerical simulation was 14.24 bar, and the maximum explosion pressure rising rate was 5.06 bar/ms. The maximum explosion pressure was 13.0 bar, and the maximum explosion pressure rising rate was 5.2 bar/ms as reported by Zhe *et al.* [6]. The numerical simulation results were consistent with the experimental results. Because the ignition delay time set in numerical simulation deviated from the experiment, the rise time of numerical simulation was later than that of the experiment.

Table 3. Simulation results compared with experimental data from [5]

Model [bar]	Experimental [bar]				
	1	2	3	4	5
14.24	15.60	15.76	15.15	14.78	15.02

Pressure piling

The explosion process of connected structures implemented by Singh and Ogungbemide was reproduced through numerical simulation [11, 17]. As displayed in fig. 5, in the initial stage, through the partition of the connection of the two flameproof cavities, the initial pressure of flameproof Chamber A and flameproof Chamber B was 1 bar. In the middle of the explosion cavity in the left end cover of Chamber A after ignition, the flame propagated in a spherical

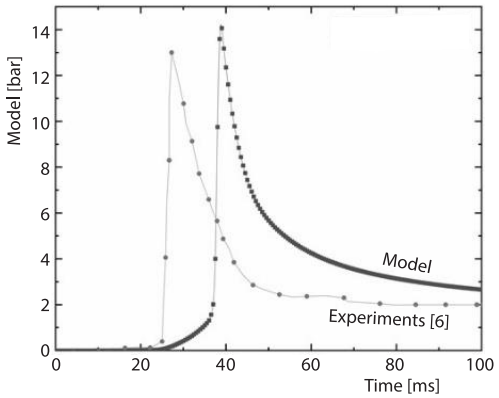

Figure 4. Comparison of explosion pressure curve correlation results for the numerical simulation and experiments

shape in the direction of flameproof Chamber A. During transmission, because of viscous resistance [18], flameproof Chamber A exhibited a flame front along the direction of flameproof Chamber B. Thus, flame propagation was accelerated. As the pressure of flameproof chamber A gradually increased, the generated pressure difference promoted unburned gas to spread to flameproof Chamber B before the flame through the small hole of the orifice [19], and the gas in flameproof Chamber B was compressed. At this stage, the pressure of flameproof Chamber B changed, and the pressure value was higher than the atmospheric pressure. When the flame reached the small hole of the orifice, the flame was sprayed toward flameproof Chamber B through the small hole in a jet form because the small hole disturbed the unburned combustible gas, enhanced the turbulence intensity, intensified the combustion reaction, and increased the combustion speed. The combustible gas in flameproof Chamber B burned rapidly [20], and the pressure in flameproof Chamber B increased rapidly (the rising speed is considerably greater than that of flameproof Chamber A), and soon exceeded the pressure in flameproof Chamber A. Next, the flame in flameproof Chamber B propagated back toward flameproof Chamber A. When the combustible gas in flameproof Chamber B was burned, some unburned combustible gas was present in flameproof Chamber A.

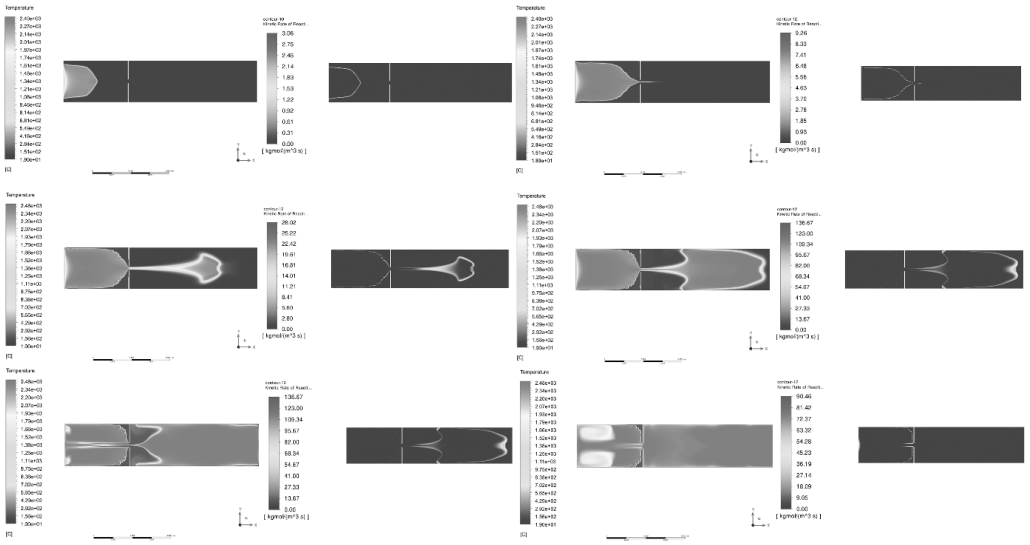

Figure 5. Flame propagation structure at different simulation times

Analysis of explosion curve of flameproof enclosure A

A flameproof enclosure under various maximum explosion pressure and maximum pressure rise speed, maximum explosion index, and maximum explosion pressure rise time is

presented in tab. 4. When the orifice hole diameter range was 10-30 mm, the flameproof enclosure of the explosion pressure increased with the increase in the hole diameter and maximum pressure rise speed, and the maximum explosion index increased. The maximum explosion pressure rise time decreased with the increase in the hole diameter. When the hole diameter of the orifice was 30 mm, the explosion pressure of flameproof Chamber A was at the maximum, the pressure rise speed was maximum, the corresponding maximum explosion index was maximum, and the maximum explosion pressure arrival time was the minimum. When the hole diameter of the orifice was 45 mm, the explosion pressure of flameproof Chamber A was greater than that of flameproof Chamber B, and the time required to reach the maximum explosion pressure should be equal, which indicated that no pressure piling occurred.

Table 4. Explosion parameters of flameproof enclosure under different working conditions

Working conditions	Hole diameters	A					B				
		P_m	$(dp/dt)_{max}$	K_{max}	t_p	t_{pm}	P_m	$(dp/dt)_{max}$	K_{max}	t_p	t_{pm}
1	10mm	5.66	120.4	29.93	47.0	100.2	8.96	963.4	239.44	9.3	80.5
2	15mm	6.19	164.2	40.81	37.7	93.8	9.09	977.4	242.91	9.3	72.5
3	20mm	6.98	261.4	64.97	26.7	80.0	8.62	836.9	207.99	10.3	69.9
4	25mm	7.46	428.7	106.55	17.4	71.3	8.22	805.9	200.28	10.2	65.7
5	30mm	7.69	732.4	182.01	10.5	63.4	8.39	830.7	206.45	10.1	60.1
6	45mm	8.61	441.6	109.73	19.5	77.3	7.79	338.6	84.17	23.0	78.2

Figure 6 displays the curve of the explosion pressure of flameproof chamber A with pressure piling. The small hole considerably affected the combustion of the combustible gas in flameproof Chamber A. With the increase in the diameter of the small hole, the maximum explosion pressure of flameproof chamber A also increased, and the time required to reach the maximum explosion pressure increased because the larger the hole diameter, the smaller was the surface area of the Orifice, the less heat loss was caused by combustion, and the greater was the explosion pressure. The smaller the hole diameter was, the less the combustion in cavity A was affected by the combustion in cavity B. The larger the hole diameter was, the greater the reverse flow of gas in cavity A was [21]. With the influence of turbulence, the combustion of the combustible gas in cavity A accelerated and the time required to reach the maximum explosion pressure was shorter.

The effect of the hole on the pressure of flameproof Chamber A should be considered when designing the flameproof enclosure because the maximum explosion pressure of flameproof Chamber A reached 7.69 bar when the hole diameter was 30 mm after the addition of the orifice.

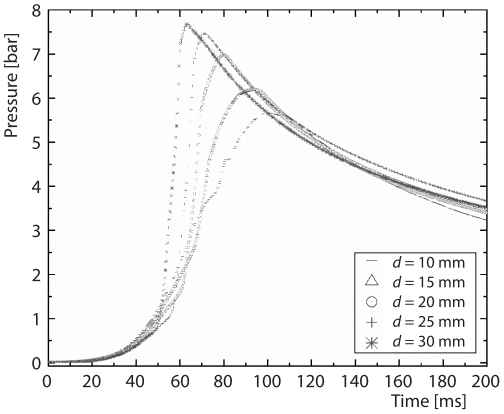

Figure 6. Explosion curve of flameproof chamber A when pressure piling

Analysis of explosion curve of flameproof enclosure

Figure 7 displays the curve of the explosion pressure of the flameproof enclosure for six working conditions. When the hole diameters were 10 mm, 15 mm, 20 mm, 25 mm, and 30 mm, the maximum explosion pressure of flameproof Chamber B was higher than that of flameproof Chamber A. The explosion pressure curve of flameproof Chamber A was gentler that that of flameproof Chamber B, and the explosion pressure curve of flameproof Chamber B peaked, which indicated that pressure piling occurred. When the diameter of the hole was 45 mm, the pressure of flameproof Chamber B was close to that of flameproof Chamber A, and the pressure curve tended to be consistent, which indicated that no pressure piling occurred.

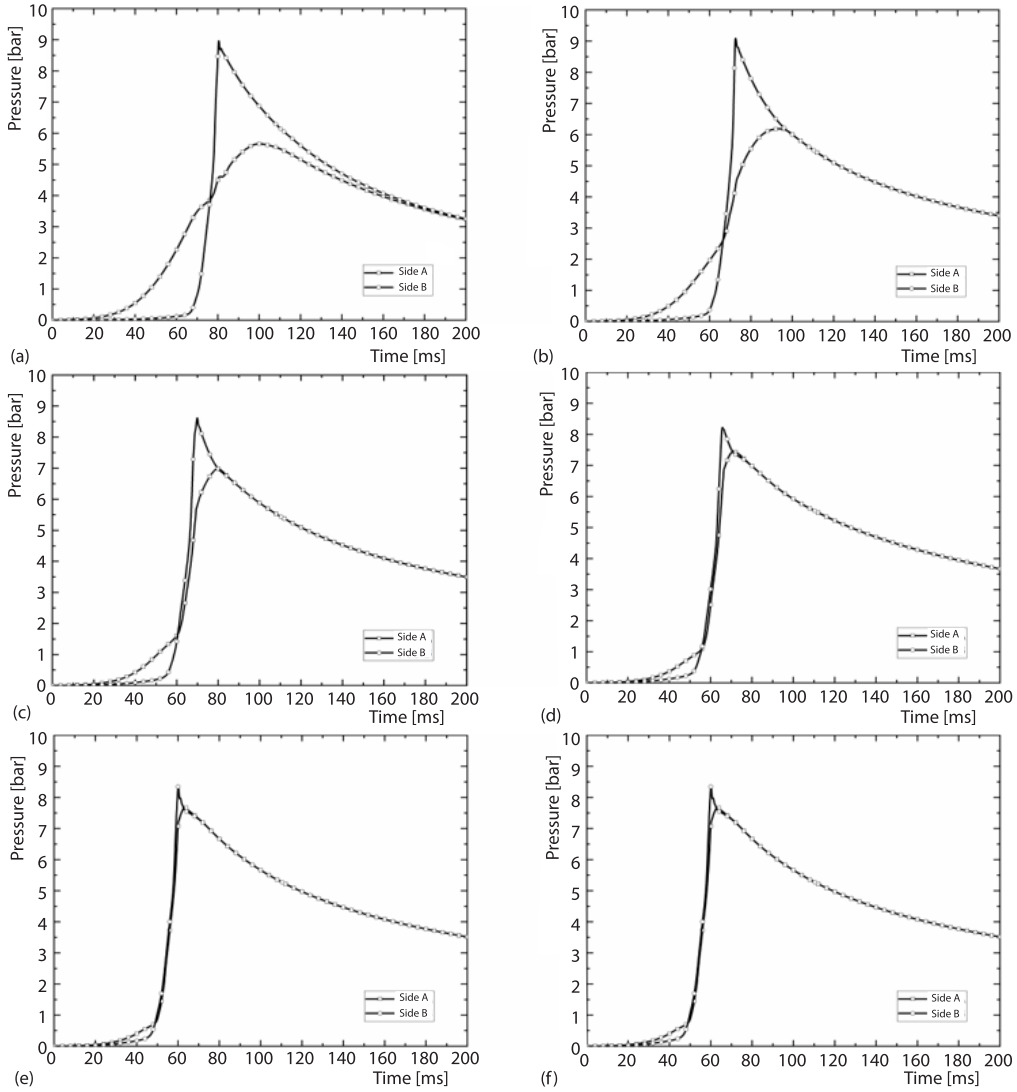

Figure 7. Explosive pressure curve of flameproof enclosure for different orifice hole diameters; (a) d = 10 mm, (b) d = 1 mm, (c) d = 20 mm, (d) d = 25 mm, (e) d = 30 mm, and (f) d = 45 mm

The figure reveals that with pressure piling, the initial pressure of the combustible gas in flameproof Chamber B before ignition was greater than the atmospheric pressure, which resulted in pre-pressurization. The diameter of the small hole considerably affected the maximum pressure ratio between flameproof Chamber B and flameproof Chamber A, and the pressure ratio between flameproof Chamber B and flameproof Chamber A increased as the diameter of the small hole decreased. When the diameter of the hole was 10 mm, the differential pressure ratio between the two chambers was the largest. The explosion pressure ratio is displayed in fig. 8.

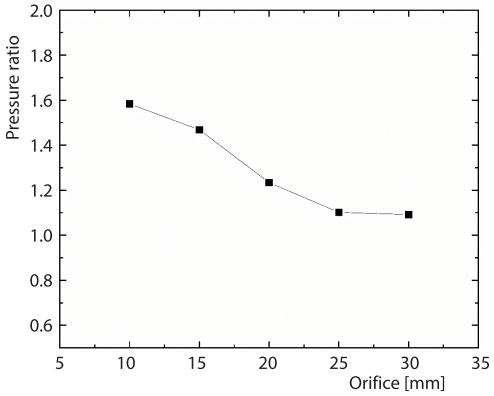

Figure 8. Explosive pressure ratio of flameproof Chambers B and A for different hole diameters

The maximum explosion pressure, pressure rise speed, explosion index, rise time of the maximum explosion pressure, and arrival time of the maximum explosion pressure of flameproof Chamber B were analyzed under various working conditions. Table 4 reveals that the maximum explosion pressure of flameproof Chamber B generally exhibited an upward trend as the diameter of the small hole decreased. The maximum pressure rise speed and the maximum explosion index also exhibited a rising trend because when the flame passed through the small hole, the flame surface was elongated because of the obstruction of the orifice plate. The smaller the aperture of the small hole was, the longer the flame stretched, the smaller the flame passage was, the faster the acceleration was, the greater the turbulence intensity was [21], and the earlier the time at which the maximum explosion pressure was reached. For the same working conditions, the maximum pressure rise velocity and the maximum explosion index of flameproof Chamber B were higher than those of flameproof Chamber A. The rise time of the maximum explosion pressure and the arrival time of the maximum explosion pressure were less than those of flameproof Chamber A. When the diameter of the hole was 15 mm, the maximum explosion pressure of cavity B reached the maximum value, the maximum pressure rise speed was the highest, the corresponding explosion index was also the highest, and the maximum explosion pressure rise time was the shortest.

Analysis of pressure piling mechanism

As mentioned, when the flame propagated through the orifice to flameproof Chamber B, the initial pressure of explosion Chamber B was higher than that of the atmospheric pressure. Additionally, the combustible gas within cavity B was compressed, and the flame sprayed under a strong disturbance condition. The effect of the combination of the phenomena revealed that for the flameproof enclosure combustion in B as the turbulence model, the explosion pressure value for explosion Chamber B was considerably higher than thermodynamic values.

The ignition time and the pre-pressurization value of the combustible gas in flameproof Chamber B with pressure piling are presented in tab. 5. Tables 4 and 5 reveal that when the diameter of the hole was 30 mm, the pre-pressurization value of flameproof Chamber B was the highest, but the maximum explosion pressure of flameproof Chamber B was not the highest. The pressure piling of flameproof Chamber B was caused by the combined action of preloading and turbulence. Pre-pressurization and explosion strength are two primary mechanisms affecting pressure piling [22].

Table 5. Pre-pressurization values of flameproof Chamber B with different hole diameters at ignition time

Working conditions	Hole diameters	Ignition time	Pre-pressurization values
1	10 mm	54.0	0.08
2	15 mm	50.0	0.12
3	20 mm	50.0	0.19
4	25 mm	45.0	0.18
5	30 mm	44.9	0.27

Pre-pressurization

Unburned gas-flowing from flameproof Chamber A to flameproof Chamber B through the small hole in the baffle plate increased the initial pressure of flameproof Chamber B, which ignited flameproof Chamber B at an initial pressure that was higher than the atmospheric pressure, as displayed in figs. 7(a)-7(e). The initial pressure considerably influenced the explosion pressure. With the increase in the initial pressure, the explosion pressure increased linearly, and this linear relationship can be explained using the formula of the explosion pressure [23]:

$$P_{\mathrm{m}} = \frac{T_{\mathrm{m}} n_m}{T_0 n_0} P_0 \tag{4}$$

where P_{m} is the maximum explosion pressure of the gas, P_0 – the initial pressure of the gas, T_{m} – the maximum temperature of the gas after the explosion, T_0 – the initial temperature of the gas, n_m – the number of moles of gas after the explosion, and n_0 – the number of moles of the gas before the explosion.

According to eq. (4), the maximum explosion pressure was proportional to the initial pressure, and the initial pressure increases, and the maximum explosion pressure also increased.

Turbulence intensity

As displayed in fig. 5, the flame was sprayed to flameproof Chamber B through the small hole in a jet form, which disturbed the unburned combustible gas, enhanced the turbulence intensity, and intensified the combustion reaction. When flameproof Chamber B was ignited, eddy currents were generated, the flame spread into a turbulent flame, the combustion speed was accelerated, and the explosion pressure increased rapidly. Figure 9 displays the turbulent kinetic energy of the combustible gas combustion in flameproof Chamber B at the ignition moment of flameproof Chamber B. As displayed in fig. 9, when the hole diameter was 15 mm, the turbulent kinetic energy of the combustible gas combustion in flameproof Chamber B was the highest, and the maximum explosion pressure of flameproof Chamber B was the highest. The hole diameter was within the range 15-30 mm. The turbulent kinetic energy of combustible gas in flameproof Chamber B decreased, the chemical reaction time of the combustible gas increased, and the combustion speed increased.

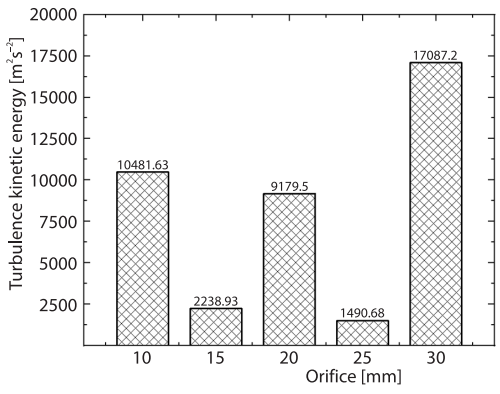

Figure 9. Turbulence kinetic energy at the hole at ignition time for flameproof Chamber B under different working conditions

As mentioned, the explosion parameters of flameproof Chamber B were affected by the pre-pressurization and turbulent kinetic energy at the ignition moment, and the pre-pressurization value of flameproof Chamber B at the ignition moment was related not only to the compression effect of the combustible gas in flameproof Chamber A after ignition but also to the fluid-flowing from flameproof Chamber B to flameproof Chamber A. Benedetto *et al.* used Br_t to represent the ratio of the reaction time to the release time in turbulent combustion [22]:

$$\mathrm{Br}_t = 0.21\sqrt{\frac{E_0}{\gamma_u}}\frac{u}{x}\frac{AC_0}{V^{2/3}S_l\left(E_0-1\right)} \tag{5}$$

where E_0 is the expansion factor, γ_u – the specific heat ratio for the unburned fuel at initial condition, u – the discharge coefficient, x – the turbulence factor, A – the vent ratio (the tube section), C_0 – the ambient sound speed, V – the vessel volume, and S_l – the laminar burning velocity at ambient condition.

The larger the turbulence intensity, the higher is the value x is, the shorter is the gas combustion time, the shorter is the corresponding release time, the smaller is Br_t, and the higher is the pressure peak value of flameproof Chamber B. Conversely, the peak pressure of flameproof Chamber B was lower.

Significance of industrial design

This study provided considerable insight into design of flameproof enclosures with double-cavity-connected structures. The study revealed that pressure piling can be avoided by changing the hole diameters of the orifice. The objective of this study was to ensure that no pressure piling occurred in the flameproof enclosure when the flame-roof hole was 45 mm. In industrial design, explosion-proof electrical manufacturers can finalize explosion-proof products using the results of this study. Furthermore, an effective double chamber connected structure of a flameproof enclosure can be designed. Thus, the study was separated into two independent cavities to avoid pressure piling.

Conclusions

In this study, numerical simulation was performed to study the effect of small holes on the flameproof enclosure of a double-cavity-connected structure. The influence of pressure piling on the maximum explosion pressure, maximum pressure rise velocity, and maximum explosion index was studied. The main findings of this study are as follows.

- The small hole between the two cavities of the double-cavity-connected structure of a flameproof enclosure increased the explosion pressure of flameproof Chamber A.
- The larger the diameter of the small hole was, the greater the explosion pressure of flameproof Chamber A was.
- The pressure ratio between two cavities decreased with the increase in the hole diameter.
- For a double-cavity-connected flameproof enclosure, when the hole diameter was designed with the appropriate value, pressure piling did not occur.
- Double-cavity-connected flameproof enclosures avoid pressure piling and were added to reduce turbulence, which could be achieved by changing the hole diameter of the orifice.
- The small hole between the two cavities of the double-cavity-connected structure of a flameproof enclosure constituted a sufficient condition for the pressure piling. For a single chamber flameproof enclosure, the arrangement of electrical components should avoid forming small holes in the internal channel.

Acknowledgment

This research was funded by CNOOC Energy Technology and Services Limited, grant number TJY-2021-FB-01.

The authors would like to thank all the reviewers who participated in the review and MJEditor (www.mjeditor.com) for its linguistic assistance during the preparation of this manuscript.

Nomenclature

Br_t – turbulent Bradley number, [–]
$(dp/dt)_{max}$ – maximum rate of explosion pressure rise, [bars^{-1}]
d – orifice hole diameter, [mm]
K_{max} – explosion pressure index $=(dp/dt)_{max} \times v^{1/3}$, [barms^{-1}]
P_0 – initial pressure, [bar]
t_p – maximum pressure rise time, [ms]
t_{pm} – time to reach maximum pressure, [ms]
V – vessel volume, [L]

References

[1] ***, Explosive atmospheres – Part 1: Equipment protection by flameproof enclosures “d”, International Electrotechnical Commision: Geneva, Switzerland, 2018
[2] ***, International Electrotechnical Vocabulary(IEV)-Part 426:Explosive Atmospheres,, International Electrotechnical Commission: Geneva, Switzerland, 2020
[3] Benedetto, A. D., *et al.*, The Mitigation of Pressure Piling by Divergent Connections, *Process Safety Progress*, *24* (2010), 4, pp. 310-315
[4] Razus, D., *et al*., Transmission of an Explosion between Linked Vessels, *Fire Safety Journal*, *38* (2003), 2, pp. 147-163
[5] Zhang, J., *et al.*, Experimental Study on Explosion Pressure Testing for Cylindrical Flameproof Products, *Journal of Safety Science and Technology*, *15* (2019), 05, pp. 80-84
[6] Zhe, J. U., *et al*., The Superposition Impact of Orifice Structure of Flameproof Enclosure on Explosion Pressure, *Safety in Coal Mines*, *45* (2014), 05, pp. 219-221
[7] Bartknecht,W., *Dust Explosions Course, Prevention, Protection*, Dust Explosions, Course, Prevention, Protection, Springer, Verlag, Berlin, Germany, 1981
[8] Razus, D., *et al.*, Transmission of an Explosion through a Narrow Channel, *Rivista dei Combustibili*, *51* (1997), 3, pp. 126-136
[9] Zhen, *et al.*, Experimental Study of the Initial Pressure Effect on Methane-Air Explosions in Linked Vessels, *Process Safety Progress*, *37* (2018), 1, pp. 86-94
[10] Ogungbemide, D., *et al*., Numerical Modelling of the Effects of Vessel Length-to-Diameter Ratio (L/D) on Pressure Piling, *Journal of Loss Prevention in the Process Industries*, *70* (2021), 1-2, 104398
[11] Ogungbemide, D. I., A CFD Study of the effects of Pipe Bending Angle on Pressure Piling in Coal Dust Explosions in Interconnected Vessels, *Fire Safety Journal*, *128* (2022), 103540
[12] Kumar, *et al*., Dynamic Response and Effect of Apertures on Explosion Parameters of Flameproof Apparatus, *Journal of Loss Prevention in the Process Industries*, *33* (2015), Jan., pp. 245-249
[13] Krause, T., *et al.*, Investigations of Static and Dynamic Stresses of Flameproof Enclosures, *Journal of Loss Prevention in the Process Industries*, *49* (2017), Sept., pp. 775-784
[14] Munro, J., *et al*., Flame Transmission at Extremely Low Temperatures when Pressure Piling is Present, *IEEE Transactions on Industry Applications*, *PP* (2016), 99, pp. 1-1
[15] Chen, F., Effect of Termination Compartment on Explosion Pressure of Flameproof Motor, *Safety in Coal Mines*, *50* (2019), 10, pp. 129-131
[16] Cammarota, F., *et al.*, Experimental Analysis of Gas Explosions at Non-Atmospheric Initial Conditions in Cylindrical Vessel, *Process Safety and Environmental Protection*, *88* (2010), 5, pp. 341-349
[17] Singh, J., Gas Explosions in Inter-Connected Vessels: Pressure Piling, *Process Safety and Environmental Protection*, 72 (1994), 4, pp. 220-228
[18] Kurdyumov, V. N., Matalon, M., Flame Acceleration in Long Narrow Open Channels, *Proceedings of the Combustion Institute*, *34* (2013), 1, pp. 865-872
[19] Kurydumov, V. N., Matalon, M., Self-Accelerating Flames in Long Narrow Open Channels, *Proceedings of the Combustion Institute*, *35* (2015), 1, pp. 921-928

[20] A, R.H., *et al.*, Effects of position and frequency of obstacles on turbulent premixed propagating flames, *Combustion and Flame*, *156* (2009), 2, pp. 439-446
[21] Rogstadkjernet, L., *Combustion of Gas in Closed, Interconnected Vessels: Pressure Piling,* University of Bergen, Bergen, Norway, 2004
[22] Benedetto, A. D., Salzano, E., The CFD Simulation of Pressure Piling, *Journal of Loss Prevention in the Process Industries*, *23* (2010), 4, pp. 498-506
[23] Li Run-zhi., *et al.*, Influence of Environmental Temperature on Gas Explosion Pressure and Its Rise Rate, *Explosion and Shock Waves*, *33* (2013), 4, pp. 415-419

Paper submitted: June 13, 2022
Paper revised: August 15, 2022
Paper accepted: August 19, 2022